ELSEVIER

Journal of Photochemistry and Photobiology A: Chemistry 107 (1997) 35–42

Journal of PHOTOCHEMISTRY AND PHOTOBIOLOGY A: CHEMISTRY

Electron transfer in donor–acceptor pair in modified α-chymotrypsin. Effect of microviscosity, macroviscosity and local polarity

Olga V. Belonogova [a,*], Gertz I. Likhtenstein [b], Victor I. Krinichnyi [a]

[a] *Institute of Chemical Physics, Russian Academy of Sciences, Chernogolovka, Moscow Region, 142432, Russia*

[b] *Department of Chemistry, Ben Gurion University of the Negev, P.O. Box 653.84105, Beer-Sheva, Israel*

Received 4 July 1996; accepted 2 January 1997

Abstract

Electron transfer was studied within a donor–acceptor pair in spin-labelled α-chymotrypsin with the methionine-192 group modified with 4-iodacetamide-2,2,6,6-tetramethylpiperidine-1-oxyl. The effects of temperature ($T = 200$–300 K), viscosity and humidity on the rate constant of photoreduction of the nitroxide fragment (acceptor) by the protein tryptophan residue in the excited singlet state (donor) were investigated. In parallel, the dynamics of the microenvironment in the vicinity of the nitroxide and tryptophan were studied by electron spin resonance (ESR) spectroscopy (X-band and high-resolution 2 mm waveband) and fluorescence techniques respectively. The apparent polarity of the microenvironment was also determined by ESR and fluorescence techniques. It was shown that the changes in the rate constant of photoreduction correlate with the changes in the parameters of the local dynamics of the donor–acceptor pair microenvironment (correlation time $\tau_c \leq 10^{-7}$ s) recorded by ESR spectroscopy. From the data on the local dynamics and polarity, the energetic profile of the photoreduction was determined. The role of local dynamics in the stabilization of photoseparated charges by time-dependent polar solvation (dynamic adaptation) is discussed. © 1997 Elsevier Science S.A.

Keywords: Electron transfer; ESR spectroscopy; Fluorescence technique; Rate constant; Spin-labelled α-chymotrypsin

1. Introduction

Electron transfer in proteins has been studied extensively in the past decade. Recent results from several groups have been reviewed [1–12]. In spite of recent progress, little is known about the factors affecting electron transfer in proteins. A protein globule possesses a number of specific features, such as a mosaic of local dynamics and polarity. The principal shortcoming of recent investigations appears to be the underestimation of these specific properties.

A start has been made to overcome this shortcoming by the study of donor–acceptor (D–A) hybrid pairs consisting of a photoactive luminescent chromophore as the donor and a nitroxide radical as the acceptor. This system enables the kinetics of electron transfer and the local dynamics and polarity to be monitored at the same time and space [13–15].

Electron spin resonance (ESR) spectroscopy enables the irreversible photoreduction of the nitroxide fragment to be followed and the radical dynamic behaviour to be studied. Indeed, the rotational diffusion correlation times (τ_c) and activation parameters (E_{eff} and $\Delta S^{\ddagger}_{eff}$) of nitroxide radicals in different media (liquids and polymer solutions) are close to the corresponding parameters recorded by nuclear magnetic resonance (NMR) spectroscopy and dielectric relaxation. Thus the values of τ_c for nitroxide radicals characterize quantitatively the dynamics of the spin label microenvironment. Luminescence techniques can be used to monitor the reversible reduction of the nitroxide by recording the fluorescence or phosphorescence quenching of the donor. The mobility of the dipoles in the vicinity of the chromophore group in the excited singlet state can be estimated from the relaxation shift of the fluorescence spectra [16–21].

The two techniques (ESR and luminescence) can be employed to estimate the local polarity in the vicinity of the acceptor and donor groups. It has been shown in a model system [18] that the hyperfine interaction constants of the spin labels, A_{zz} and A_{iso}, depend on the dielectric constant in the vicinity of the labels and on hydrogen bond formation. Therefore these parameters can be used to measure the micropolarity of the environment. The relaxation shift of the fluorescence spectra ($\Delta\nu$) also depends on the dielectric constant of the environment and, after calibration of this parameter ($\Delta\nu$), reflects, to a certain extent, the polarity of the environment [17].

* Corresponding author. Fax: +7 096 515 3588.

PII S1010-6030(97)00015-4

The dynamic state of protein globules can also be estimated by Mössbauer spectroscopy. This method allows the measurement of the amplitudes and frequencies of Mössbauer probes introduced into different parts of the protein globule [21].

The purpose of this study is to investigate, using ESR, luminescence and Mössbauer spectroscopy, the correlation between the rate constant of electron transfer within a D–A pair in modified α-chymotrypsin (α-ChT) and the parameters of microdynamics and micropolarity of the system. The intrinsic tryptophan group of the protein in the excited singlet state is the donor and the nitroxide residue attached to the methionine group is the acceptor. The two groups are localized in the vicinity of the enzyme active centre [22].

2. Materials and methods

2.1. Preparation and equipment

α-ChT was purchased from "Olayne" Company (Latvia) and purified by filtering through a Sephadex G-25 column equilibrated with 0.001 N HCl. 4-Iodacetamide-2,2,6,6-tetramethylpiperidine-1-oxyl (**1**) ("Reanal", Hungary) was used as spin label

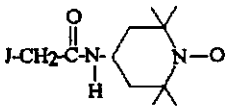

α-ChT was modified by spin label **1** at methionine-192 (Met-192) as described elsewhere [23]. The degree of modification (measured by a comparison of the integral intensity of the ESR spectra at 77 K for spin-labelled α-ChT and for a standard ethanol solution of spin label **1**) is approximately 30%, in good agreement with Kosman [23].

Solutions of different viscosity were prepared by adding sucrose of chemical grade. The solution viscosity was determined at room temperature using the method described in Ref. [24].

The modification of the amino acid residues on the α-ChT surface by Mössbauer atoms (^{57}Fe) was carried out by the method given in Ref. [19], resulting in approximately three iron atoms per protein molecule.

The procedure of moistening of the protein samples was performed using the method described in Ref. [25]. The samples were lyophilized and held for 2–6 days at a certain degree of relative humidity $P_{rel} = P/P_s$, where P is the water vapour pressure above a sulphuric acid solution and P_s is the water vapour pressure above pure water at a given temperature.

ESR spectra were recorded with an SE/X-2544 Radiopan spectrometer (X-band) and a high-resolution 2 mm waveband spectrometer with a cylinder cavity of H_{011} type and a constant magnetic field of 5 T [26]. In both cases, the radiospectrometers were equipped with a temperature controller. Quartz capillaries of 2 mm in diameter (for the X-band spectrometer) and 0.5 mm in diameter (for the 2 mm waveband spectrometer) were placed in the cavity of the spectrometer. The X-band ESR spectra were recorded with the following instrument settings: modulation frequency, 100 kHz; modulation amplitude, 0.3 mT; microwave power, 20 mW; sweep width, 10 mT. The 2 mm waveband ESR experiments were performed at a modulation frequency of 100 kHz, microwave magnetic field $H_1 = 20$ μT and a sweep width of 10 mT.

The g factor calibration was performed using an Mn^{2+} standard with a hyperfine constant $a = 8.74$ mT and $g = 2.00102$.

Luminescence measurements were performed on solid samples under controlled humidity conditions using a modified "Aminco-Bowman" spectrofluorometer equipped with a temperature controller [13,14].

2.2. Photochemical experiments

Photochemical experiments with powders or solutions of spin-labelled α-ChT, placed in a quartz capillary of 2 mm in diameter, were carried out in an ESR cavity with illumination by a 200 W mercury lamp at a wavelength $\lambda > 300$ nm. The intensity of illumination was insufficient to produce photochemical conversion of spin label **1** in aqueous solution. The photochemical conversion of the nitroxide fragment of spin-labelled α-ChT in the powder state was 60% for $P_{rel} = 0.95$ at 298 K.

The efficiency of acceptor photoreduction was estimated using ESR spectra from the disappearance rate of the nitroxide. The apparent first-order rate constant of nitroxide photoconversion (k_T^{ph}) was calculated from the experimental kinetic curves at each temperature and the relative degree of humidity (P_{rel}). The relative value $k_{rel} = k_T^{ph}/k_{298}^{ph}$, where k_{298}^{ph} is the rate constant at 298 K, was taken as a quantitative measure of the photoreactivity of the system under investigation.

The electron transfer obeys first-order kinetics up to 60% photoconversion. This indicates that only one type of donor takes part in this process. This donor is probably tryptophan-215 which, according to the X-ray model [22], is localized in the hydrophobic pocket of α-ChT at a distance of approximately 0.8 nm from the Met-192 group modified with the nitroxide label. In the presence of oxygen, the kinetic curves have a complicated character. It is probable that oxygen oxidizes the photoreduced nitroxide and decreases the reaction quantum yield. It has been shown [13] that the initial portion of the kinetic curve is identical in the presence or absence of oxygen; therefore the experiments were carried out in the presence of oxygen, using the initial portion of the kinetic curve for rate constant calculation. Thus the photoconversion is attributed to the photoreduction of the nitroxide by tryptophan-215 in the excited singlet state with the subsequent reduction of tryptophan-215 by a neighbouring protein group.

2.3. Data analysis

In the case of fast rotation of the nitroxide, the correlation times (τ_c) were calculated by the formulae [18]

$$\tau_c^{(-)} = (\sqrt{h_0/h_-} - 1)\Delta H_0/3.6\times10^9 \text{ (s)} \quad (1)$$

$$\tau_c^{(\pm)} = (\sqrt{h_+/h_-} - 1)\Delta H_+/1.5\times10^9 \text{ (s)} \quad (2)$$

where ΔH_0 and ΔH_+ are the linewidths (G) of the components of the X-band ESR spectra of the spin label with $m=0$ and $m=+1$ respectively and h_+, h_- and h_0 are the amplitudes of the low-field, high-field and central components of the spectrum respectively.

In the region of slow motion, the τ_c values were calculated by the formula

$$\tau_c = a(1 - A_{zz}/A'_{zz})^b \quad (3)$$

where A_{zz} and A'_{zz} represent the hyperfine splitting of the Z components of the X-band ESR spectra for τ_c and $\tau_c \to \infty$ respectively. In our case, $a = 8.52\times10^{-10}$ and $b = -1.16$ for the Brownian diffusion model [27].

In the case of the high-resolution 2 mm waveband ESR spectra, the values of τ_c were calculated according to Ref. [28].

The characteristic time (τ_r) of orientational relaxation of the dipoles in the vicinity of tryptophan in the excited singlet state was calculated by [13]

$$\tau_r = (\nu_0^f - \nu^f)\tau_f/(\nu^f - \nu_\infty^f) \quad (4)$$

where τ_f is the lifetime of the excited state, ν^f is the frequency of the maximum of the tryptophan fluorescence spectrum and ν_0^f and ν_∞^f are the limiting values of ν^f at $\tau_r \to 0$ and $\tau_r \to \infty$ respectively.

The microviscosity (η^{SL}) in the vicinity of the nitroxide fragment of the spin label was estimated from the value of the correlation time (τ_c) by the Stokes–Einstein equation using the radical radius $R_0 = 0.4$ nm. The microviscosity (η^M) in the vicinity of the Mössbauer probe ^{57}Fe attached to the α-ChT globule surface was evaluated from the data on the probability of recoil-less resonance absorption of a γ quantum (f'). The value of f' is determined from the intensity of the Mössbauer spectra [29]. This method has been used for microviscosity estimation in the vicinity of Mössbauer atoms [30].

The micropolarity in the vicinity of the nitroxide fragment of spin-labelled α-ChT was evaluated by comparison of its magnetic spectroscopic parameters g_{xx} and A_{zz} with those of spin label 1 in organic solvents at low temperature where all molecular motions in the samples are very slow. The magnetic spectroscopic parameters were obtained by analysis of the ESR spectra in the 2 mm waveband.

The comparison of the position of the fluorescence maximum ν^f of tryptophan in α-ChT and in organic solvents was used to estimate the apparent dielectric constant (ϵ_{app}^f) of the microenvironment of the chromophore.

3. Results

3.1. Effect of temperature on the photoreduction rate constant and the molecular dynamics

The temperature dependences of the relative rate constants (k_{rel}) of photoreduction of the nitroxide fragment of spin-labelled α-ChT in a lyophilized dry sample with a relative humidity of $P_{rel} = 0.04$ and in a wet sample with $P_{rel} = 0.95$ are presented in Fig. 1. The figure shows that, in the dry sample, the rate of photoreduction is very low in the temperature range 220–295 K. Moistening of the sample leads to an increase in k_{rel} at $T > 240$ K. In a control sample with free spin label 1 in water solution, the radical is stable on illumination. Photoconversion of the nitroxide radical in solution does not occur because of the lack of an electron source. Therefore this experiment supports the supposition that, under the given experimental conditions (temperature, illumination, time), the only cause of radical disappearance is photoreduction in the presence of an electron donor. In our case, the photoconversion plausibly proceeds via electron transfer from the excited singlet state of α-ChT tryptophan (donor) to the nitroxide fragment (acceptor). A similar process has been observed in a hybrid molecule consisting of 1-dimethylaminonaphthalene-5-sulphonate (donor) and a nitroxide radical (acceptor) in solution [13] and also when incorporated into the hydrophobic cavity of bovine serum albumin [12].

The temperature dependences of the hyperfine splitting of the spin label ESR spectrum in the X-band (A_{zz}), the fluorescence maximum of tryptophan (λ) and the logarithm of the probability of recoil-less γ quantum absorption ($\ln f'$) in dry and wet samples of spin-labelled α-ChT are given in Fig. 2 and Fig. 3. The temperature dependences of the dynamic parameters, namely the correlation time of rotational diffusion of the spin label (τ_c) calculated from the ESR spectra in the X-band and high-resolution 2 mm waveband, the characteristic time of orientational relaxation of the dipoles in the vicinity of α-ChT tryptophan in the excited

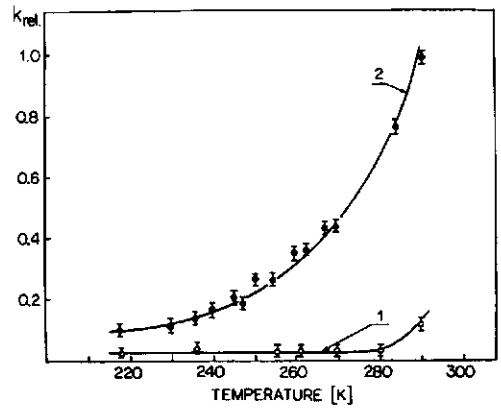

Fig. 1. Temperature dependence of the relative rate constant of photoreduction (k_{rel}) for spin-labelled α-ChT at relative humidities of 0.04 (1) and 0.95 (2).

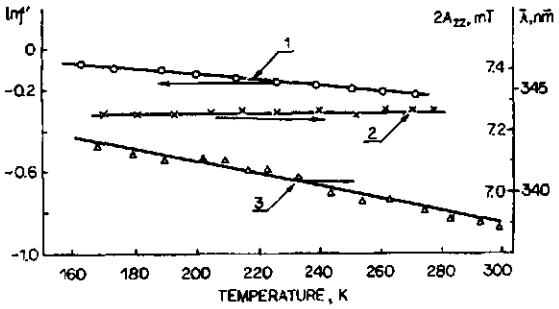

Fig. 2. Temperature dependence of the experimental parameters of the Mössbauer spectrum ($\ln f'$) from ^{57}Fe attached to the α-ChT surface (1), the maximum position of the α-ChT tryptophan fluorescence spectrum (λ) ($\lambda = c/\nu^{f}$, where $c = 3\times10^{10}$ cm s^{-1}) (2) and the hyperfine splitting of the X-band ESR spectrum ($2A_{zz}$) (3) for spin-labelled α-ChT at a relative humidity $P_{rel} = 0.04$.

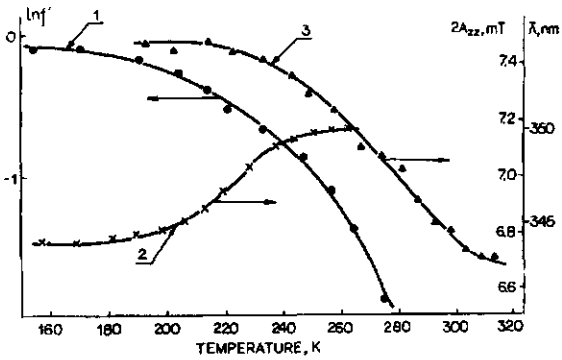

Fig. 3. Temperature dependence of the experimental parameters of the Mössbauer spectrum ($\ln f'$) from ^{57}Fe attached to the α-ChT surface (1), the maximum position of the α-ChT tryptophan fluorescence spectrum (λ) (2) and the hyperfine splitting of the X-band ESR spectrum ($2A_{zz}$) (3) for spin-labelled α-ChT at a relative humidity $P_{rel} = 0.95$.

singlet state (τ_r) and the microviscosity parameter (η^M) in the vicinity of the Mössbauer probe ^{57}Fe attached to the α-ChT globule surface, are presented in Fig. 4.

It is known [31] that α-ChT contains eight tryptophan groups localized on the surface and inside the protein globule. These groups can be divided into two types according to their fluorescence properties: $\lambda_f^1 = 330$–332 nm (exposed in water) and $\lambda_f^2 = 340$–342 nm (localized in the interior region), with the lifetimes of the excited states $\tau_f^1 = 2.1$ ns and $\tau_f^2 = 4.5$ ns respectively. The temperature dependence of λ results in an average picture. Therefore the estimation of $\tau_r = f(T)$ (see Eq. (4)) was carried out for τ_f^1 and τ_f^2. It is seen from Fig. 4 that a change in τ_r is observed at $T > 180$ K for both type 1 ($\tau_r < 3$ ns) and type 2 ($\tau_r < 6$ ns) tryptophans, whereas, in the same samples, an increase in the radical photoreduction rate constant (Fig. 1, curve 2) is observed only at higher temperature. Thus the motion of the dipoles in the vicinity of the tryptophan group with $\tau_r < 3$ ns does not correlate with the electron transfer.

The same conclusion can be drawn from the temperature dependence of $\ln f'$ (Fig. 4, curve 4). The iron atoms are bound to the α-ChT surface residues and their Mössbauer spectra give an average picture of motion of the surface groups. A marked variation of $\ln f'$ is revealed at temperatures $T > 200$ K. This implies that the low-amplitude oscillation of the ^{57}Fe Mössbauer probe cannot promote radical photoconversion.

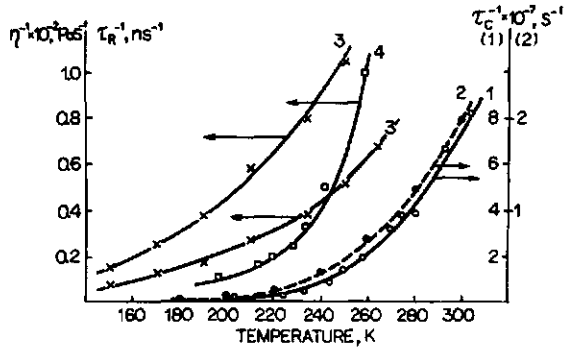

Fig. 4. Temperature dependence of the correlation times (τ_c) of rotational diffusion of spin label 1 in spin-labelled α-ChT in the X-band (1) and high-resolution 2 mm waveband (2) ESR spectra, the characteristic times (τ_r) of orientational relaxation of the dipoles in the vicinity of α-ChT tryptophan (3 and 3' for $\tau_f^1 = 2.1$ ns and $\tau_f^2 = 4.5$ ns respectively) and the microviscosity parameters (η^M) (4), calculated from the dependence $f'(T)$, at a relative humidity $P_{rel} = 0.95$.

As observed in Fig. 4, in wet samples, the temperature region in which the spin label rotates with $\tau_c \leq 2\times10^{-7}$ s coincides roughly with the region in which the value of k_{rel} (Fig. 1) varies markedly. In dry samples, both processes (radical photoreduction and motion with $\tau_c \leq 2\times10^{-7}$ s) are not observed. The suppression of photoreduction in dry samples ($P_{rel} = 0.04$) is attributed to the slow dynamics (see Fig. 2), rather than to the weak penetration of light into dry powder-like samples. This is supported by three independent methods (ESR, Mössbauer spectroscopy and the relaxation shift method; the latter method is sensitive only to surface motions). These methods show the absence of motions with nanosecond frequencies in the temperature region in which the photoreduction rate is very slow.

3.2. *Effect of viscosity on the photoreduction rate constant and molecular dynamics*

Fig. 5 presents the dependences of k_{rel} and τ_c on the medium viscosity for an aqueous solution of spin-labelled α-ChT; the values of k_{rel} and τ_c were calculated from the same

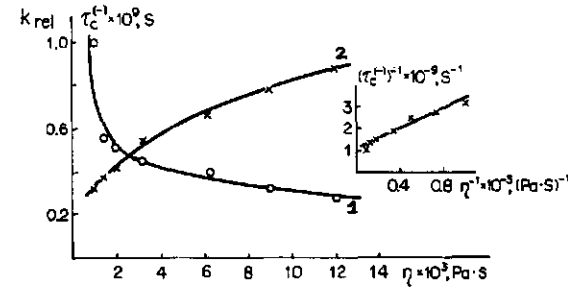

Fig. 5. Dependence of the relative rate constant of photoreduction (k_{rel}) (1) and τ_c (2) of spin-labelled α-ChT in aqueous solution on the medium viscosity. Inset (a): correlation between parameters τ_c and η^{-1} in the same samples.

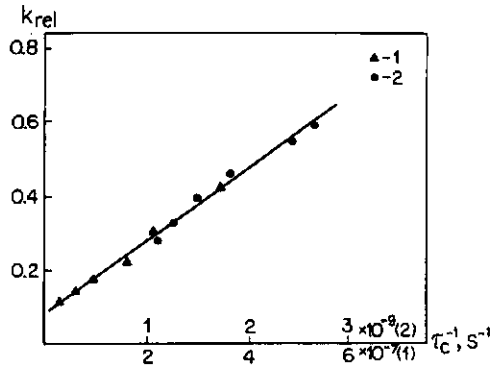

Fig. 6. Dependence of the relative rate constant (k_{rel}) and τ_c^{-1} of spin-labelled α-ChT at $P_{rel}=0.95$ (1) and in aqueous solution (2) on the macroviscosity values $\eta=10^{-3}$–10^{-2} Pa s.

ESR spectra. The value of τ_c depends linearly on the medium viscosity within a certain interval of viscosity (Fig. 5(a)). This justifies the use of τ_c for the characterization of the microenvironment dynamics.

As observed in Fig. 6, for wet samples and aqueous solutions the value of k_{rel} correlates with the dynamic parameter τ_c^{-1}. This indicates that the relatively high-amplitude mobility of the water–protein matrix with $\tau_c \leq 10^{-7}$ s in the vicinity of the D–A pair promotes the electron transfer process.

It is important that the simultaneous use of nitroxide radicals and spin labels provides the unique possibility to measure the electron transfer rate and the parameters of the microenvironment polarity and dynamics at the same time and space without a detailed knowledge of the tested system structure. The presence of unlabelled α-ChT in the tested samples should not influence the correlation of the electron transfer rate constant with the parameters of the molecular dynamics and polarity of the microenvironment.

3.3. Estimation of the molecular dynamics parameters from the data obtained by 2 mm waveband ESR

More detailed information on the motion of the nitroxide fragment of spin-labelled α-ChT was obtained by 2 mm waveband ESR spectroscopy. According to the formula $h\nu = g\beta H$, the registration of the ESR spectra at higher microwave frequencies results in a better spectral resolution of peaks with different g factors (for details, see Ref. [26]). A model ESR spectrum of the nitroxide radical recorded by a 2 mm waveband ESR spectrometer is given in Fig. 7. In the dry sample, a marked change in the shape of the ESR spectrum of spin-labelled α-ChT was detected only at $T>290$ K. At $T=300$ K, $\tau_c=6\times10^{-7}$ s, the activation energy of radical rotation $E=73.5$ kJ mol^{-1} and the pre-exponential factor $\nu_0=1.7\times10^{18}$ s^{-1}. The apparent local microviscosity η^{SL} was estimated to be 72 Pa s. In the wet spin-labelled α-ChT sample at $T>260$ K, the X and Z components of the spectrum are broadened and shifted to the centre of the spectrum, whereas the position of the Y component remains unchanged (Fig. 7). This can be explained as a result of the rotation of the nitroxide fragment with $\tau_c \leq 6\times10^{-7}$ s around the Y axis.

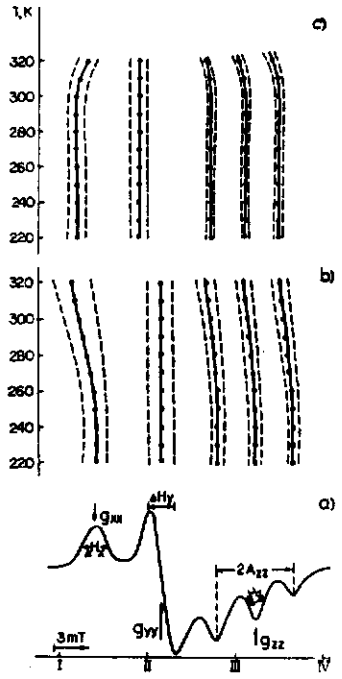

Fig. 7. The 2 mm waveband ESR spectrum of spin-labelled α-ChT at $P_{rel}=0.95$ and $T=220$ K (a); position (———) and half-width (- - -) of the ESR spectrum components vs. temperature at $P_{rel}=0.95$ (b) and $P_{rel}=0.04$ (c); I–IV, positions of the Mn^{2+} standard components.

According to a calculation at 300 K, $\tau_c=1.2\times10^{-7}$ s, $E=25$ kJ mol^{-1}, $\nu_0=2.4\times10^{10}$ s^{-1} and $\eta^{SL}=14.4$ Pa s.

The microviscosity η^{SL} and apparent microviscosity η^{M}, calculated from the temperature dependence of f' (probability of recoil-less resonance absorption of a γ quantum) (Fig. 3) by the method given in Ref. [29], are presented in Table 1.

3.4. Estimation of the micropolarity

The magnetic constants of a sample of α-ChT modified by spin label **1** and of a solution of spin label **1** in organic solvents of different polarity are presented in Fig. 8. It can be seen that an increase in the polarity of the microenvironment of spin label **1** in the model system causes a gradual decrease in the g_{xx} values and an increase in the A_{zz} values. This observation provides unequivocal evidence for the formation of a π–σ radical complex with molecules of the medium [35].

The similar values of the magnetic constants of spin label **1** in α-ChT ($P_{rel}=0.04$) and ethanol show that the polarity and structure of the environment of the N–O group are identical in these matrices. A deviation of the g_{xx}–A_{zz} correlation from that of the model system can be explained by a conformational strain of the radical structure caused by the protein environment

Moistening of spin-labelled α-ChT leads to a gradual change in the magnetic constant of spin label **1**. At a relative humidity $P_{rel}=0.95$, the A_{zz} value of the radical is equal to that of the radical in methanol with a dielectric constant $\epsilon_{app}^{SL}=33$.

Table 1
Data on the apparent microviscosity and micropolarity in spin-labelled α-ChT

Relative humidity	T (K)	Area, label	Microviscosity η (Pa s)	Micropolarity (ϵ_{app})
0.04	140	N–O	–	24 [a]
	300		72 [e]	
0.95	140			33 [a]
	300		14.4 [e]	45 [d]
0.95	140	Trp		2 [b]
	300			54 [c]
0.95	140	Ser		2 [b]
	300		100 [f]	54 [c]

[a] Calculated from the data of 2 mm waveband ESR Fig. 8.
[b] Ref. [32].
[c] Calculated from Fig. 3 as described in Ref. [17].
[d] Calculated from the data of X-band ESR [33,34].
[e] Calculated from the data of 2 mm waveband ESR.
[f] Calculated from the data of $\ln f'(T)$ [29].

An analysis of the relaxation shifts of tryptophan (Fig. 3) permits an estimation of the polarity of the microenvironment of α-ChT tryptophan. The relaxation shifts for α-ChT and model systems with various polarities were compared [17]. As a result, an apparent value of the dielectric constant (ϵ^f_{app}) in the vicinity of the tryptophan donor group was estimated. Data on the microviscosity and micropolarity for spin-labelled α-ChT are summarized in Table 1.

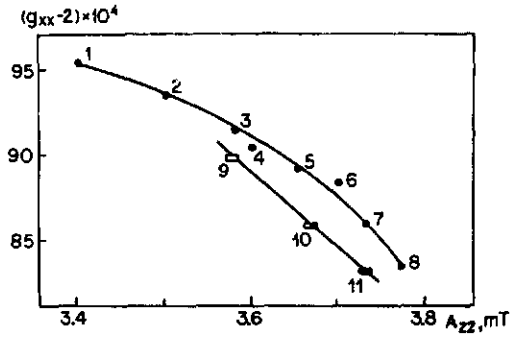

Fig. 8. Correlation between g_{xx} and A_{zz} for spin label 1 in frozen (140 K) (●) toluene (1), isobutanol (2), ethanol (3), water–ethanol mixture with 0.25 (4), 0.5 (5) and 0.66 (6) H_2O content, methanol (7), water–glycerol (10 : 1 v/v) mixture (8); spin-labelled α-ChT at 0.04 (9), 0.65 (10) and 0.95 (11) relative humidity.

4. Discussion

4.1. The kinetic scheme of irreversible photoreduction

The results given above can be considered within the framework of the following scheme of photoconversion in the D–A (tryptophan–nitroxide radical) pair [13]

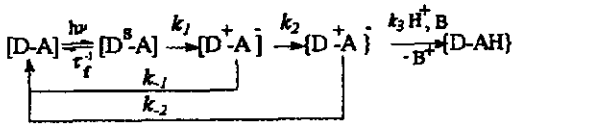

In our case, this scheme is represented as follows

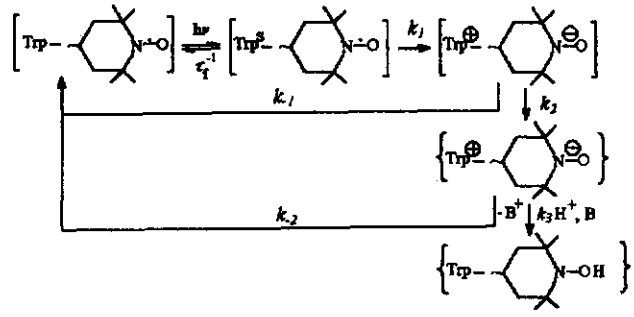

where $h\nu$ is the quantum of exciting light, τ_f is the donor (tryptophan) fluorescence lifetime, k_1 and k_{-1} are the rate constants of direct and reverse intramolecular electron transfer, k_2 is the solvation rate constant and k_{-2} is the reverse charge transfer in the molecule after solvation. Trp^S is the donor molecule in the excited singlet state, B is the protein group which donates an electron to the cation Trp^+ with the formation of the final product of photoreduction D–AH and the brackets and braces denote the initial and final configurations of the unrelaxed and relaxed microenvironments respectively.

An analysis of the scheme by the method of steady concentration gives the following value of the apparent rate constant of photoreduction

$$k_{app} = h\nu k_1 k_2 k_3 [H^+] / (k_1 + \tau_f^{-1})(k_2 + k_{-1})(k_3[H^+] + k_{-2}) \quad (5)$$

and the quantum yield

$$\varphi = k_1 k_2 k_3 [H^+] / (k_1 + \tau_f^{-1})(k_2 + k_{-1})(k_3[H^+] + k_{-2}) \quad (6)$$

In compliance with Eq. (6), the yield of the final product D–AH can be expected to be high at $k_1 \geq \tau_f^{-1}$, $k_{-1} \leq \tau_r^{-1}$ ($k_2 = \tau_r^{-1}$), $\tau_r^{-1} \geq k_1$, $k_1 \geq k_{-1}$ and, as a consequence, at $\tau_r^{-1} \geq \tau_f^{-1}$.

4.2. Estimation of the photoreduction free energy

The free energy of the reaction can be calculated by the formulae [36]

$$\Delta G = I_D - [E_A + E_D^S] - e^2/\epsilon(R_A + R_D) + \Delta G_{solv} \quad (7)$$

or

$$\Delta G = E_{1/2}(D/D^+) - [E_{1/2}(A^-/A) + E_D^S] - e^2/\epsilon(R_A + R_D) + \Delta G_{solv} \quad (8)$$

where I_D is the ionization potential of the donor, E_A is the electron affinity of the acceptor (nitroxide), E_D^S is the excitation energy of the donor (tryptophan) to the singlet state, ΔG_{solv} is the free energy of solvation of $[D^+-A^-]$, R_A and R_D are the radii of the acceptor and donor groups, $E_{1/2}(D/D^+)$ and $E_{1/2}(A^-/A)$ are the standard oxidation potential (vs. saturated calomel electrode (SCE)) for the donor and standard reduction potential (vs. SCE) for the acceptor and ϵ is the apparent dielectric constant of the medium.

The following experimental data were used for the calculation of $\Delta G_{300\,K}$ for the D–A pair (tryptophan–nitroxide) in the absence of polar solvation: $E_D^S = 3.6$ eV (calculated from the temperature dependence of λ, Fig. 3), $E_{1/2}(D/D^+) = 1.26$ eV and $E_{1/2}(A/A^-) = -0.3$ eV for the nitroxide radical [36,37].

The value of $e^2/\epsilon(R_D + R_A)$ is equal to 0.03 eV for $R_A = 0.4$ nm, $R_D = 0.45$ nm [38] and $\epsilon = 54$ (see Table 1). Taking into account these parameters, the value of $\Delta G_{300\,K} = -2$ eV was calculated using Eq. (8).

The energy of solvation of $[D^+-A^-]$ can be evaluated by the Born equation

$$\Delta G_{solv} = e^2/2[R_D^{-1}(1 - 1/\epsilon_D) + R_A^{-1}(1 - 1/\epsilon_A)] \quad (9)$$

where ϵ_D and ϵ_A are the apparent local dielectric constants in the vicinity of the donor and acceptor respectively. (The values of ϵ_A and ϵ_D were taken from Table 1.)

The free energy of solvation can be calculated for donor (tryptophan) and acceptor (nitroxide) separately. For tryptophan, $\Delta G_{solv} = 0.8$ eV and 1.57 eV at 140 K and 300 K respectively. For the nitroxide radical, $\Delta G_{solv} = 1.74$ eV and 1.76 eV at 140 K and 300 K. Thus the overall change in the solvation free energy $\Delta(\Delta G_{solv}^1)$ with decreasing temperature from 300 to 140 K is equal to -0.8 eV.

The most probable secondary donor B is the serine group (Ser-214) for which $I_B = 9.19$ eV and $R_B = 0.13$ nm [38,39]. According to Eq. (7), the free energy for electron transfer from serine to tryptophan$^{(+)}$ in the absence of solvation is 1.29 eV. The overall change in the free energy of solvation of this pair is $\Delta(\Delta G_{solv}^2) = -3.55$ eV with decreasing temperature from 300 to 140 K (calculated using Eq. (9)). These results are presented in Fig. 9.

According to the energy diagram (Fig. 9), the only processes thermodynamically allowed for the dry sample at low temperature with very slow orientational relaxation (when $\tau_r^{-1} \ll k_{-1} \ll \tau_f^{-1}$) are electron transfer from D to A and

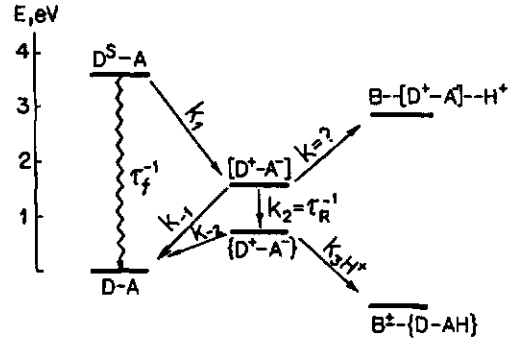

Fig. 9. Energy diagram of the reaction under investigation.

recombination of "frozen" ion–radical pairs $[D^+-A^-]$. Further reduction of D^+ is energetically unfavourable in these conditions and favourable when $\tau_r^{-1} > k_{-1}$ and $\tau_r^{-1} \geq \tau_f^{-1}$.

The theoretical predictions given above have been confirmed experimentally. A marked increase in the rate of irreversible photoreduction of the nitroxide fragment is observed at a temperature and humidity at which the spin label method detects mobility of the water–protein matrix in the vicinity of the photoreduction zone with a correlation time $\tau_c \leq 10^{-7}$ s and an apparent microviscosity $\eta = 14.4$ Pa s. An appropriate correlation time of the environment mobility does not appear to be the only requirement for the reaction under study. As shown in Fig. 3, a low-amplitude oscillation of the Mössbauer probes on the α-ChT surface with $\tau_c \leq 10^{-7}$ s and a local orientation of the dipoles in the vicinity of the excited singlet state of tryptophan with $\tau_r \leq 3$ ns are observed at temperatures shifted by 40–60 K to the low-temperature region relative to the temperature of significant enhancement of the radical photoreduction rate.

The basic requirements for effective electron transfer, in addition to appropriate orbital overlap [3], are as follows:

1. favourable thermodynamics, which are dependent on the local micropolarity which, in turn, is dependent on the local dynamics of the microenvironment;
2. competition between relaxation processes with τ_r^{-1} and recombination of the separated charges with a rate constant k_{-1}.

5. Conclusions

The analysis of the data presented in this paper leads to the conclusion that the molecular dynamics of the microenvironment make an important contribution to the micropolarity and hence to the efficiency of electron transfer within D–A pairs in proteins. This contribution is provided by the build-up of an energy profile favourable for orientational relaxation which stabilizes the photoseparated charges $[D^+-A^-]$ involved in further chemical conversion. This conclusion is consistent with the general principle of the dynamic adaptation of the protein matrix environment to the structure of a reaction complex in biochemical and chemical reactions [18,21,40–43].

Acknowledgements

This work was supported in part by the Russian Foundation for Fundamental Research (grant N 96-04-49799). The authors express their sincere gratitude to Dr A.V. Kulikov for help with the ESR experiments and valuable criticisms and Dr V.R. Vogel for useful discussions and valuable criticisms.

References

[1] A.I. Berg, P.P. Knox, A.A. Kononenko, G.N. Frolov, I.N. Chrymova, A.B. Rubin, G.I. Likhtenstein, V.I. Goldanskii, F. Parak, M. Bucl, R. Mössbauer, Molekulyarnaya Biologiya 13 (1979) 81–89.
[2] I.D. Zusman, Chem. Phys. 49 (1980) 295–302.
[3] R.A. Marcus, N. Sutin, Biochem. Biophys. Acta 811 (1985) 265–322.
[4] I.E.T. Iben, D. Braunstein, W. Doster, H. Frauenfelder, M.K. Hong, J.B. Johnsson, S. Cuck, P. Ormos, A. Schulte, P.J. Steinbach, A.H. Xie, R.D. YOung, Phys. Rev. Lett., 62 (1989) 1916–1923.
[5] G.L. McLendon, Acc. Chem. Res. 21 (1988) 160–167.
[6] I. Rips, J. Jortner, J. Chem. Phys. 88 (1988) 818–822.
[7] B.E. Bowler, T.J. Meade, S.L. Mayo, J.H. Richards, H.B. Gray, J. Am. Chem. Soc. 111 (1989) 8757–8759.
[8] J.M. Nocek, N. Liang, S.A. Wallin, A.G. Mauk, H.M. Hoffmann, J. Am. Chem. Soc. 112 (1990) 1623–1625.
[9] A.I. Burstein, A.A. Jharikov, Chem. Phys. 152 (1991) 23–30.
[10] P. Siddarth, R.A. Marcus, J. Chem. Phys. 97 (1993) 13 078–13 082.
[11] A. Harriman, V. Heitz, M. Ebersole, H. Willigen, J. Phys. Chem. 98 (1994) 4982–4989.
[12] V.R. Vogel, E.T. Rubtsova, G.I. Likhtenstein, K. Hideg, J. Photochem. Photobiol. A: Chem. 83 (1994) 229–236.
[13] I.M. Bystrjak, G.I. Likhtenstein, A.I. Kotelnikov, H.O. Hankovsky, K. Hideg, Zh. Fiz. Khim. 60 (1986) 2796–2802.
[14] I.M. Bystrjak, G.I. Likhtenstein, A.I. Kotelnikov, Zh. Fiz. Khim. 60 (1986) 2803–2807.
[15] E.T. Rubtsova, V.R. Vogel, G.I. Likhtenstein, Biofizika 38 (1993) 211–216.
[16] N.G. Bakhshiev, Spectroscopy of Intermolecular Interaction, Nauka, Leningrad, 1972.
[17] E.A. Burstein, Luminescence of protein chromophores (model investigation), in: Ju.A. Vladimirov (Ed.), Biofizika 6 (1976) 1–213.
[18] G.I. Likhtenstein, Spin Labeling Methods in Molecular Biology, Wiley-Interscience, New York, 1976.
[19] O.V. Belonogova, E.N. Frolov, N.N. Illustrov, G.I. Likhtenstein, Molekulyarnya Biologiya 13 (1979) 567–575.
[20] G.I. Likhtenstein, A.I. Kotelnikov, Molekulyarnaya Biologiya 17 (1983) 505–518.
[21] G.I. Likhtenstein, Chemical Physics of Redox Metalloenzyme Catalysis, Springer Verlag, Heidelberg, 1988.
[22] T.A. Steitz, R. Henderson, D.M. Blow, J. Mol. Biol. 46 (1969) 337–349.
[23] D.J. Kosman, J. Mol. Biol. 67 (1972) 247–259.
[24] D.F. Othmer, S.J. Silver, Sugar 43 (1948) 32–36.
[25] V.Ja. Rosljakov, Ju.I Khurgin, Biokhimija 37 (1972) 404–407.
[26] V.I. Krinichnyi, J. Biochem. Biophys. Methods 23 (1991) 1–30.
[27] S.A. Goldman, G.V. Bruno, J.H. Freed, J. Phys. Chem. 76 (1972) 1858–1860.
[28] A.A. Dubinsky, O.Ja. Grinberg, V.I. Kurochkin, L.G. Oransky, O.G. Poluektov, Ja.S. Lebedev, Teoretich. (i) Eksp. Khimija 17 (1981) 231–236.
[29] K.V. Shaitan, A.B. Rubin, Molekulyarnaya Biologiya 14 (1980) 1323–1335.
[30] G.I. Likhtenstein, S.M. Bystrjak, A.I. Kotelnikov, Khim. Fiz. 9 (1990) 697–705.
[31] E.A. Burstein, N.S. Vedenkina, M.N. Ivkova, Photochem. Photobiol. 18 (1973) 263–279.
[32] P. Douzou, Cryobiochemistry. An Introduction, Academic Press, London, New York, San Francisco, 1977.
[33] C.L. Hamilton, H.M. McConnell, Spin labels, in: A. Rich, N. Davidson (Eds.), Structural Chemistry and Molecular Biology, Freeman, San Francisco, CA, 1968, pp. 115–149.
[34] A.N. Kuznetsov, The Method of Spin Probes, Nauka, Moscow, 1976.
[35] A.L. Buchachenko, Complexes of Radical and Molecular Oxygen with Organic Molecules, Nauka, Moscow, 1984.
[36] A.K. Chibisov, Uspechy Khimii 50 (1981) 1169–1196.
[37] L.B. Volodarskii, I.A. Grigoriev, S.A. Dikanov, V.A. Resnikov, G.I. Shukin, Imidasolin Nitroxyl Radicals, Nauka, Novosibirsk, 1988.
[38] A.L. Lehninger, Biochemistry. The Molecular Basis of Cell Structure and Function, Worth Publishers, New York, 1972.
[39] V.N. Kondrat'ev, The Energy of Chemical Bond Breaking. The Ionization Potential and Electron Affinity, Nauka, Moscow, 1974.
[40] G.I. Likhtenstein, Biofizika 11 (1966) 24–32.
[41] L.A. Blumenfeld, R.M. Davidov, Biochem. Biophys. Acta 547 (1979) 255–286.
[42] G.I. Likhtenstein, Stud. Biophys. 111 (1986) 89–100.
[43] R. Lumry, R.B. Gregory, Free energy movements in protein reactions: concepts, complications and compensation, in G.R. Welch (Ed.), The Fluctuating Enzymes, Wiley, New York, 1986, pp. 3–185.